Optimized Peptide Amount and Activity for ^{90}Y-Labeled DOTATATE Therapy

Peter Kletting[1], Thomas Kull[1], Christian Maaß[2], Noeen Malik[1], Markus Luster[3], Ambros J. Beer[1], and Gerhard Glatting[2]

[1]*Department of Nuclear Medicine, Ulm University, Ulm, Germany;* [2]*Medical Radiation Physics/Radiation Protection, Universitätsmedizin Mannheim, Medical Faculty Mannheim, Heidelberg University, Mannheim, Germany; and* [3]*Klinik für Nuklearmedizin, Universität Marburg, Marburg, Germany*

In peptide receptor radionuclide therapy with ^{90}Y-labeled DOTATATE, the kidney absorbed dose limits the maximum amount of total activity that can be safely administered in many patients. A higher tumor-to-kidney absorbed dose ratio might be achieved by optimizing the amount of injected peptide and activity, as recent studies have shown different degrees of receptor saturation for normal tissue and tumor. The aim of this work was to develop and implement a modeling method for treatment planning to determine the optimal combination of peptide amount and pertaining therapeutic activity for each patient. **Methods:** A whole-body physiologically based pharmacokinetic (PBPK) model was developed. General physiologic parameters were taken from the literature. Individual model parameters were fitted to a series (n = 12) of planar γ-camera and serum measurements (^{111}In-DOTATATE) of patients with meningioma or neuroendocrine tumors (NETs). Using the PBPK model and the individually estimated parameters, we determined the tumor, liver, spleen, and red marrow biologically effective doses (BEDs) for a maximal kidney BED (20 $Gy_{2.5}$) for different peptide amounts and activities. The optimal combination of peptide amount and activity for maximal tumor BED, considering the additional constraint of a red marrow BED less than 1 Gy_{15}, was individually quantified. **Results:** The PBPK model describes the biokinetic data well considering the criteria of visual inspection, the coefficients of determination, the relative standard errors (<50%), and the correlation of the parameters (<0.8). All fitted parameters were in a physiologically reasonable range but varied considerably between patients, especially tumor perfusion (meningioma, 0.1–1 $mL \cdot g^{-1} \cdot min^{-1}$, and NETs, 0.02–1 $mL \cdot g^{-1} \cdot min^{-1}$) and receptor density (meningioma, 5–34 $nmol \cdot L^{-1}$, and NETs, 7–35 $nmol \cdot L^{-1}$). Using the proposed method, we identified the optimal amount and pertaining activity to be 76 ± 46 nmol (118 ± 71 μg) and 4.2 ± 1.8 GBq for meningioma and 87 ± 50 nmol (135 ± 78 μg) and 5.1 ± 2.8 GBq for NET patients. **Conclusion:** The presented work suggests that to achieve higher efficacy and safety for ^{90}Y-DOATATE therapy, both the administered amount of peptide and the activity should be optimized in treatment planning using the proposed method. This approach could also be adapted for therapy with other peptides.

Key Words: PBPK modeling; PRRT; ^{90}Y-DOTATATE; peptide amount; biologically effective dose (BED)

J Nucl Med 2016; 57:503–508
DOI: 10.2967/jnumed.115.164699

Peptide receptor radionuclide therapy (PRRT) is a promising method in the treatment of somatostatin receptor–expressing neuroendocrine tumors (NETs) (*1,2*). However, specific and unspecific kidney uptake limits a more effective treatment (*3*). Although, the administration of amino acids has considerably reduced unspecific uptake, the absorbed dose to the kidneys is still the most relevant hindrance to increasing the tumor absorbed dose (*3*).

A strategy to further improve the ratio of tumor to kidney absorbed dose might be adjusting the amount of injected peptide. The effect of peptide amount was investigated in animal studies (*4,5*). In humans, a strong effect of substance amount on the therapeutic index has been observed in previous work with monoclonal antibodies (*6–8*) but also peptides (*9,10*). Sabet et al. showed that saturation of tumor-binding sites requires considerably higher amounts of peptide than for those in normal tissue (*10*). Recently, we developed a pharmacokinetic model to demonstrate that different amounts of peptide for dosimetry and therapy could lead to considerably different absorbed doses (*9*). Until now, the effects of peptide amount on the tumor–to–kidney biologically effective dose (BED) ratio has not been considered in treatment planning.

Therefore, the aim of this work was to develop a treatment planning approach that allows for the estimation of the optimal combination of amount and activity for PRRT for a given maximal kidney BED. For that purpose, a whole-body physiologically based pharmacokinetic (PBPK) model was developed. The PBPK model was fitted to time–activity data derived from 12 series of planar γ-camera images and serum data. On the basis of the individually estimated parameters, the tumor, red marrow, liver, and spleen BEDs were calculated for increasing amounts of peptide using the boundary condition of a fixed BED to the kidneys of 20 $Gy_{2.5}$.

MATERIALS AND METHODS

Patients/Data

Nine patients with metastasizing NETs (n = 5) or meningioma (n = 4) were included in this study. The institutional review board (or equivalent)

Received Aug. 3, 2015; revision accepted Nov. 23, 2015.
For correspondence or reprints contact: Peter Kletting, Department of Nuclear Medicine, Ulm University, Albert-Einstein-Allee 23, D - 89081 Ulm, Germany.
E-mail: peter.kletting@uniklinik-ulm.de
Published online Dec. 17, 2015.

approved this retrospective study, and the requirement to obtain informed consent was waived. For patients 1 and 2, pretherapeutic dosimetry was conducted for 3 and 2 cycles of PRRT, respectively. In total, 12 datasets with the same sampling schedule, with an additional CT for volume measurement of the liver, kidneys, spleen, and 1 or 2 tumor lesions and with a glomerular filtration rate measurement (^{51}Cr-ethylenediaminetetraacetic acid [EDTA]), were included (Table 1). For application, ^{111}In-DOTATATE was prepared according to a protocol (*11*) that was a modified procedure as published earlier (*12*). ^{111}In-DOTATATE in phosphate-buffered saline showed a 98% or greater purity at the end of synthesis, and thus it was used directly without further purification. However, quality control was performed by radio–high-performance liquid chromatography using the same conditions as reported before for ^{90}Y-DOTA-DUPA-Pep (*11*). For pretherapeutic measurements, 116 ± 16 μg (75 ± 10 nmol) DOTATATE labeled (*12*) with (140 ± 14 MBq) ^{111}In were intravenously injected as a 51 ± 8 min infusion. Lysine and arginine (1,000 mL, 2.5% infusion) were coadministered over 2 h, beginning 0.5 h before the administration of ^{111}In-DOTATATE. Blood was drawn at 5 and 15 min; 0.5, 1, 2, and 4 h; and 1, 2, and 3 d after the end of the ^{111}In-DOTATATE infusion. Serum activity was measured using a γ-counter (Auto-γ-5003; Canberra Packard). Planar whole-body scintigraphy (anterior and posterior) with a double-head γ-camera (ECAM; Siemens) was performed at 2 and 4 h and 1, 2, and 3 d after infusion (Fig. 1). For the first measurement series (N1), the reference time was the start of the infusion. To obtain the time–activity data, ULMDOS (*13*) and NUKDOS (*14*), which contain background correction, self-attenuation, and scatter corrections according to MIRD pamphlet 16 (*15*) for conjugate view counting, were used. Regions of interest were drawn for 1 (for patients 2, 4, and 5) or 2 tumor sites, liver, left kidney, spleen, and total body. For red marrow, no direct time–activity data could be obtained. However, serum measurements and whole-body data were available (supplemental data; supplemental materials are available at http://jnm.snmjournals.org).

PBPK Model Structure

A whole-body PBPK model was developed. It describes all major physiologic and physical mechanisms—that is, distribution via blood flow, extravasation, specific binding, internalization, degradation and release, physical decay, and clearance (supplemental data). The model consists of 2 systems, 1 for labeled and 1 for unlabeled peptide (*6*). The systems are coupled by the competition for binding to free receptors and by physical decay (*6*). All physiologic parameters are assumed equal for the labeled and unlabeled substance. The organs are connected via blood flow.

For those somatostatin receptor subtype 2 (sst2)–positive organs that were not delineated, receptor densities relative to the kidney were calculated using values for regional sst2 expression reported in Boy et al. (supplemental data) (*16*). Nonlinear peptide-receptor binding was implemented. Binding to sst1 and sst3–sst5 was neglected (*17*). The internalization rates, $\lambda_{i,int}$, and the total numbers of sst2 receptors, $R_{i,0}$, were assumed to be constant over time. ^{111}In-DOTATATE was metabolized and subsequently released ($\lambda_{i,release}$) from the cell. In the model, for reasons of parsimony, the released fragments or free ^{111}In were directly excreted from the body (*18*). Equal rates were assumed for ^{90}Y-DOTATATE (*19*).

In contrast to the previously developed model (*9*), the binding of peptide to serum proteins was explicitly modeled to adequately describe serum activity for time points greater than 24 h.

Kidney uptake was modeled sst2-specific and -unspecific. All unspecific uptake mechanisms were described with the fractional flow of peptide into and out of the cells back to the serum compartment (*9*).

PBPK Model Parameters

All adjustable parameters are presented in Table 2. In the supplemental data, all equations and parameters are described. The dissociation constant and rate, K_D and k_{off}, for ^{111}In-DOTATATE (for fitting) and ^{90}Y-DOTATATE (for simulating) were set to 0.4 nmol/L (*9*) and

TABLE 1
Patient Characteristics

Patient no.	Data	Disease	Sex	Age (y)	BSA (m^2)	GFR* (L/min)	Measured volume (mL)				
							Spleen	Liver	Kidneys	Tumor 1	Tumor 2
P1	N1	Men	M	31	1.94	0.11	198	1,811	193	87	20
	N2	Men	M	32	1.92	0.12	198	1,811	193	87	20
	N3	Men	M	33	1.91	0.10	122	1,520	168	87	20
P2	N4	Men	M	31	1.99	0.12	178	1,824	185	116	—
	N5	Men	M	32	1.94	0.12	178	1,824	185	116	—
P3	N6	Men	F	56	1.94	0.090	110	1,500	125	2	0.5
P4	N7	Men	M	70	2.05	0.13	243	1,896	206	3	—
P5	N8	Net	M	76	1.98	0.032	320	4,876	147	2,520†	—
P6	N9	Net	F	33	1.81	0.092	‡	1,897	156	4	30
P7	N10	Net	M	73	1.86	0.059	146	1,804	157	111	23
P8	N11	Net	F	83	1.57	0.028	128	1,610	233	13	2
P9	N12	Net	M	78	1.81	0.050	161	1,900	156	3	15
Mean				52	1.89	0.11	180	2,023	175	40¶	
SD				22	0.12	0.12	61	910	29	44	

*Measured glomerular filtration rate (GFR) using ^{51}Cr-EDTA.
†$V_{TU,total} = V_{L,total} - V_{L,total\ average}$.
‡Splenectomy.
¶Tumor volume of patient 6 was excluded (see †).
BSA = body surface area; Men = meningioma; Net = neuroendocrine tumors.

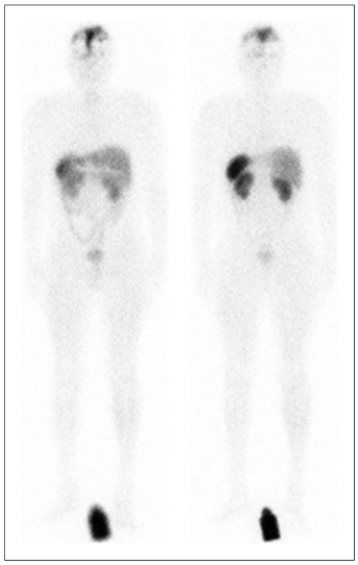

FIGURE 1. Typical biodistribution 24 h after injection. Anterior (left) and posterior (right) γ-camera images of patient 2 (N4, meningioma).

0.04 min^{-1} (supplemental data), respectively. It was assumed that only 2% of the peptide in the kidneys was filtered back to the serum due to the coadministration of amino acids (*9*). The individually measured glomerular filtration rates were used (0.66) and scaled to DOTATATE molecule size (*20*) because the macromolecular sieving coefficient of ^{51}Cr-EDTA is smaller than for DOTATATE. Cell release rates, $\lambda_{i,release}$, were estimated and assumed to be different for tumor and normal tissue. In Antunes et al. (*21*), internalization of ^{111}In-DOTATATE for tumor cells but not for kidney cells was directly measured. Thus, the average ratio (1.7) of internalization rates of kidney and tumor, estimated for other ^{111}In-labeled peptides (*21*), was used. Preliminary fits yielded tumor internalization in the order of 10^{-3} min^{-1}. Therefore, the internalization rates were fixed to $\lambda_{TU,\,int} = 0.001$ min^{-1} and $\lambda_{K,\,int} = 0.0017$ min^{-1}, respectively. The internalization rates of all other sst2-positive tissues were assumed equal to that of the kidneys. For 2 patients, a sensitivity analysis for these parameters was conducted (supplemental data).

Blood flow to the tumor is an important quantity because tissue uptake is blood-flow-limited for DOTATATE. However, in our case, the earliest organ measurement was 2 h after injection and therefore it was difficult to estimate from the data for some patients. Therefore, in models 1 and 2 the blood flow rates were set to 0.9 $mL \cdot g^{-1} \cdot min^{-1}$ for meningioma (*22*) and 1 $mL \cdot g^{-1} \cdot min^{-1}$ for NETs (*23*) and to a 10-fold-lower value, respectively. In model 3, the blood flow rates were fitted. The structure and parameters of models 1–3 were identical except for the assumption regarding the tumor perfusion.

PBPK Model Fitting and Selection

SAAMII (*24*) and SAAMII Population kinetics (versions 2.2 and 2.0; The ε Group) were used for model development with the settings as described earlier (*9*). The adjustable parameters of models 1, 2, and 3 were fitted to the time–activity data of each patient. The ratio of data points to adjustable parameters was greater than 3 for all patients (supplemental data). The corrected Akaike information criterion (*25*) was used for model selection and parameter averaging. Models with relative standard errors greater than 50% for any estimated parameter, with elements of the correlation matrix greater than 0.8 (*26*) and weights less than 10% (*27*), were not used for model averaging.

Biodistribution Simulations and BED Calculations

To automate the simulations, the model was implemented in MATLAB/Simulink (The MathWorks Inc.). The BEDs for tumor, kidneys, spleen, liver (all delineated organs), and red marrow were calculated for 2–2^{13} nmol DOTATATE in steps of factor 2 (injection duration, 60 min) for each patient. Figure 2 describes the automated workflow for the calculation of the BEDs for a fixed BED to the kidneys of 20 $Gy_{2.5}$ and a red marrow BED less than 1 Gy_{15}, as 2 cycles and a maximal cumulative BED for kidney 40 $Gy_{2.5}$ (*28*) and red marrow 2 Gy_{15} (*29*) were assumed. The simulations were conducted retrospectively. For the actual treatment of the patients, the peptide amount was not optimal, but similar amounts for pretherapeutic measurements and therapy were applied. The actual amounts and activities were used to determine the actual tumor and kidney absorbed doses. In addition,

TABLE 2
Fitted Parameters of Patient Groups

Quantity	Organ	Parameter	Meningioma			NET			Literature
			Minimum	Maximum	Median	Minimum	Maximum	Median	
Receptor concentration	Kidneys	$R_{K,0}$ ($nmol \cdot L^{-1}$)	5.7	8.8	6.5	2.3	8.7	7.1	9 ± 8*
	Spleen	$R_{S,0}$ ($nmol \cdot L^{-1}$)	7.8	16.5	9.2	3.9	18	8.7	30 ± 26*
	Liver	$R_{L,0}$ ($nmol \cdot L^{-1}$)	0.86	2.5	1.1	0.63	2.1	1.2	2 ± 1*
	Rest	$R_{REST,0}$ ($nmol \cdot L^{-1}$)	0.39	0.94	0.53	0.48	0.48	0.48	—
	Tumor	$R_{TU,0}$ ($nmol \cdot L^{-1}$)	5.0	34	17	7	35	16	34*; 8–80†
Release rate	Normal tissue	$\lambda_{NT,release}$ ($min^{-1} \cdot 10^{-4}$)	0.47	1.7	0.65	0.60	2.3	1.2	1.2–1.6‡; 0.5–1.6*
	Tumor	$\lambda_{TU,release}$ ($min^{-1} \cdot 10^{-4}$)	1.1	3.0	1.7	0	2.1	0	1.2–1.6‡; 0.4–3.0*
Volume	Tumor rest¶	$V_{TU,Total,Rest}$ (L)				0	1.2	0.10	—
Perfusion	Tumor	$f_{TU,}$ ($mL \cdot min^{-1} \cdot g^{-1}$)	0.10	1.0	0.20	0.015	1.0	0.064	0.01–1§
Linear binding rate	Serum protein	k_{Pr} ($min^{-1} \cdot 10^{-4}$)	2.1	5.6	4.3	10	23	17	—

*Data from Kletting et al. (*9*) obtained using pharmacokinetic model with simpler structure; ^{111}In-Octreoscan (dissociation constant = 5.57 nmol/L) data and smaller amounts (5.8 ± 0.4 nmol) of peptide were used.

†Calculations based on 80 $fmol \cdot 10^{-6}$ cells (*34*) and assumption of 10^{11} or 10^{12} cells L^{-1} tumor.

‡Derived from half-life (3–4 d) for release of rates of ^{111}In (*35*).

¶Volume of nondelineated, remaining tumor tissue § (*36*).

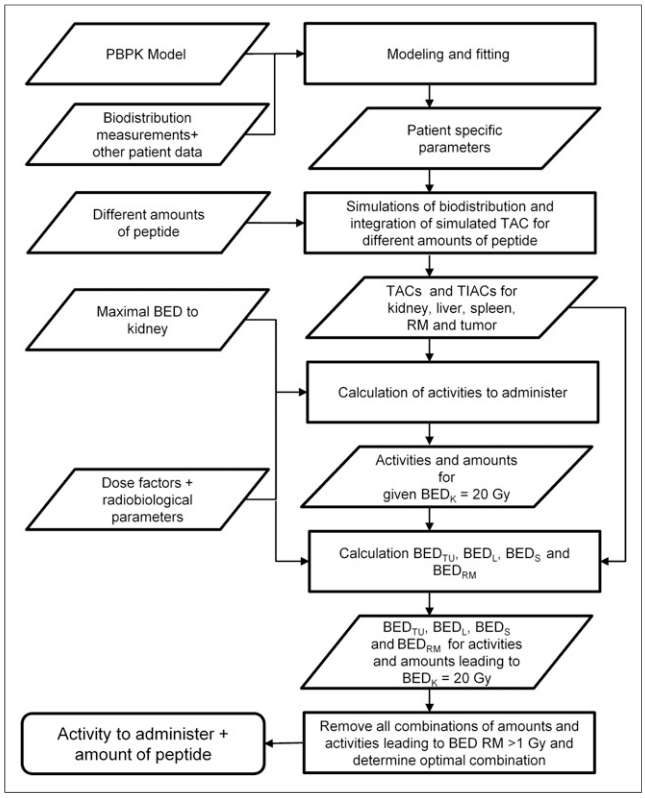

FIGURE 2. Flow diagram showing presented treatment planning approach. First, patient-specific parameters are estimated (Table 2) using PBPK model (supplemental data) and biodistribution data of individual patient (Fig. 3). Second, simulated time–activity curves (TACs) for different amounts of peptide are integrated to obtain time-integrated activity coefficients (TIACs). Third, activity to administer is calculated (Supplemental Eq. 20) for all peptide amounts for kidneys for fixed BED of 20 $Gy_{2.5}$. Fourth, with resulting activities, time-integrated activity coefficients, radiobiologic parameters, and dose factors for tumor, liver, spleen, and red marrow (RM) BEDs are computed (Figs. 4A–4C). Fifth, all combinations of amounts and activities that lead to a red marrow BED of 1 Gy_{15} are removed (Fig. 4D). Finally, optimal combination of amount and activity is determined (Fig. 4D). BED_K = kidney BED; BED_L = liver BED; BED_{RM} = red marrow BED; BED_S = spleen BED; BED_{TU} = tumor BED.

the BED of the kidneys and red marrow was calculated using the herein estimated parameters for NET patients and a standard amount (150 μg) and activity (5 GBq) from Vinjamuri et al. (*30*) for NET patients.

S values were taken from OLINDA/EXM (*31*) and scaled using CT-based liver, spleen, and kidney masses. For tumor, spheric shapes were assumed. Radiobiologic parameters α/β and μ for all organs were taken from the literature (supplemental data) (*28,32,33*).

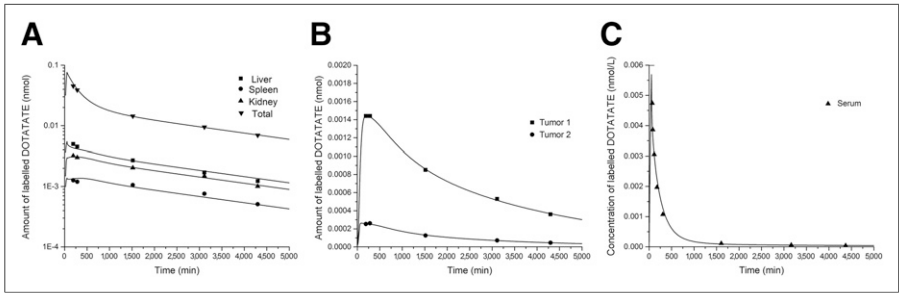

FIGURE 3. Example of typical fit (patient 1, N3): normal tissue (A), tumor (B), and serum (C).

RESULTS

Fitting and Validation

Visual inspection showed good fits. The coefficient of determination R^2 was greater than 0.9 for all curves except the spleen for N4 (0.84), N5 (0.89), N6 (0.81), N7 (0.67), and N11 (0.51); the tumor for N11 (0.80); and the kidneys for N7 (0.78). A typical fit is depicted in Figure 3. Fitted curves and estimated parameters for all measurement series are provided in the supplemental data. Models 1, 2, and 3 were most supported in 3, 1, and 8 cases, respectively. Model parameter averaging was conducted only for N8, as in all other cases only 1 model fit passed the quality criteria or had an Akaike weight ω greater than 10%. The mean values of the estimated parameters, which compare favorably to literature values, are presented in Table 2.

Simulations

Figure 4 shows the simulations for patient P2 (N5). The graphs of all other patients are presented in the supplemental data. The optimal amount and pertaining activity was 76 ± 46 nmol with 4.2 ± 1.8 GBq and 87 ± 50 nmol with 5.1 ± 2.8 GBq, for meningioma and NET patients, respectively. The results for all patients are provided in Table 3. The peptide amount affected the ratio of tumor to kidney BED strongly for measurement N2, N5, N7, and N8 and moderately for N1 and N6. For N3, N4, and N9, the effect was negligible. For the treated patients (patients 1, 2, 4, and 6), the actually used amounts were close to the optimum. However, in some patients the activity was not well selected. For the NET patients, when therapy was simulated with 5 GBq and 150 μg the median kidney BED was 11 $Gy_{2.5}$ (range, 6–19 $Gy_{2.5}$).

DISCUSSION

We developed a treatment planning approach based on a whole-body PBPK model that allowed for the estimation of the individually optimal combination of amount and activity in PRRT for a given maximal kidney BED.

The developed PBPK model described the data well, and the fitted parameter values were all in a physiologically reasonable range. The simulations showed that for patients with a high ratio of tumor to sst2 receptor density in combination with a low ratio of tumor to kidney perfusion, the peptide amount strongly influenced the BED ratio. Thus, the peptide amount is important for treatment planning. For the investigated patients, the mean optimal amount was 81 ± 47 nmol. The pertaining activities to these optimal amounts for the kidney constraint of a BED of 20 $Gy_{2.5}$ and a red marrow BED less than 1 Gy_{15} could be determined with the presented approach. The therapeutic window was wide for the actually treated patients (patients 1, 2, 4, and 6) in contrast to patients 5, 7, and 8. Figure 4 shows that along the line of allowed combinations (with kidney BED = 20 $Gy_{2.5}$ and red marrow BED < 1 Gy_{15}) from 50 nmol labeled with 4 GBq to 500 nmol with 20 GBq (not recommended due to high red marrow irradiation), the tumor BED is almost equal. Therefore, the simulations showed that the injected amounts for pretherapeutic measurements (74 ± 9 nmol) and therapy (63 ± 10 nmol) for the actually treated patients led to an almost optimal tumor-to-kidney ratio, although the effect of peptide amount was not considered. However, in some patients the optimal activity was not well selected. Thus, if the amount of peptide is not optimized for therapy,

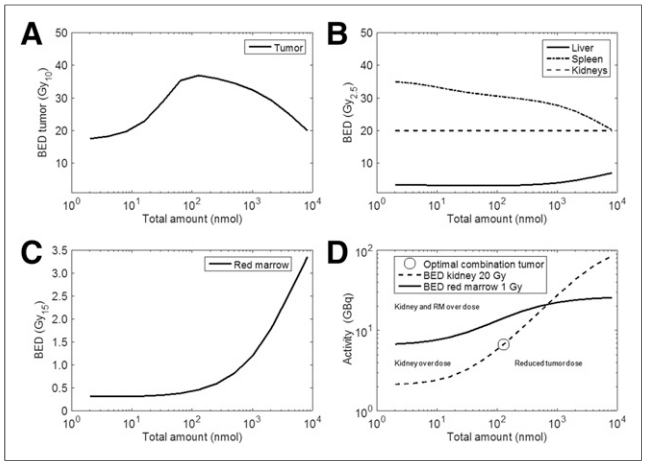

FIGURE 4. (A–C) BEDs of tumor (A) and all organs (B and C) are depicted for activity and peptide amount combinations that lead to kidney BED of 20 $Gy_{2.5}$ (D). (D) All combinations of amounts and activities that lead to kidney BED of 20 $Gy_{2.5}$ and red marrow BED of 1 Gy_{15} are depicted. All combinations along kidney BED 20 Gy curve below red marrow BED curve are allowed (radiochemical limitations are not considered). Optimal combinations for maximal tumor-to-kidney BED ratio were added. Curves divide graph in 4 fields. Estimated parameters of N5 were used. All other diagrams are show in supplemental data.

at least exactly the same amount of peptide should be used for pretherapeutic measurements (on which dosimetry is based) and therapy. For our NET patients, a standard amount and activity as reported by Vinjamuri et al. (*30*) (5 GBq with 100–200 μg) would have led to considerable undertreatment because the median kidney BED was 11 $Gy_{2.5}$ (range, 6–19 $Gy_{2.5}$), assuming maximal 3 cycles.

Compared with the recently published model (*9*), the structure of the PBPK model presented here has been refined (supplemental data), and the simulations have been extended to calculations of the absorbed doses and BEDs for all relevant organs. The herein observed effects are in agreement with our previous results.

For accurate prediction of the therapeutic biodistribution, it is necessary that the estimated physiologic parameters using individual pretherapeutic measurements and assumptions (minor fraction of unspecific kidney uptake) must be true for higher or lower peptide amounts. That necessitates the selection of proper measurement time points. The up-to-now used sampling protocol, which was adopted from radioimmunotherapy, is not optimal. For the determination of the perfusion rate, early measurements (in the range of minutes) would improve the identifiability. This work represents a general approach to quantify and include the effect of peptide amount in treatment planning. Although this effect could be adequately demonstrated and implemented using the corrected 2-dimensional data, 3-dimensional measurement techniques would

TABLE 3
Amounts, Activities, Absorbed Doses, and BEDs

			Optimal for kidney BED 20* $Gy_{2.5}$, red marrow BED < 1 Gy_{15}			Actually administered			
Patient no.	Data	Tumor	Amount (nmol)	Activity (MBq)	Tumor D (Gy) (BED [Gy_{10}])	Amount (nmol)	Activity (MBq)	Tumor D (Gy) (BED [Gy_{10}])	Kidney D† (Gy) (BED [$Gy_{2.5}$])
P1	N1	1	64	4,083	19 (20)	47	3,850	20 (21)	16 (22)
		2	32	2,954	10 (11)			11 (12)	
	N2	1	128	4,760	17 (18)	70	5,430	27 (29)	23 (36)
		2	64	3,191	9.0 (10)			15 (15)	
	N3	1	128	5,073	18 (19)	57	5,000	20 (21)	16 (22)
		2	64	3,379	12 (13)			13 (14)	
P2	N4	1	128	7,574	39 (44)	73	4,010	38 (43)	14 (20)
	N5	1	128	6,718	33 (37)	55	2,560	19 (20)	9.2 (11)
P3	N6	1	2†	1,606	4.3 (4.4)	—	—	—	—
		2	32	2,591	30 (33)				
P4	N7	1	64	4,342	25 (28)	70	5,360	30 (33)	16 (24)
P5	N8	1	128	6,217	67 (74)	—	—	—	—
P6	N9	1	32	2,674	19 (20)	70	4,000	19 (20)	15 (21)
		2	32	2,681	47 (53)			48 (54)	
P7	N10	1	128	9,596	51 (55)	—	—	—	—
		2	128	9,596	29 (30)				
P8	N11	1	64	4,915	57 (61)	—	—	—	—
		2	16	2,924	113 (133)				
P9	N12	1	128	3,665	11 (11)	—	—	—	—
		2	128	3,664	7.7 (7.8)				

*BED of 20 $Gy_{2.5}$ corresponds to approximately 14–15 Gy absorbed dose for given biokinetics.
†Radiochemical constraints were not considered.

reduce bias and uncertainty in the pharmacokinetic data and would thus allow a more accurate and precise parameter estimation.

The assumptions of a constant internalization rate (i.e., an average value for the measured and simulated time course) and constant total number of receptors (sst2 is immediately recycled back to the cell surface) had to be included as the design of the up-to-now used sampling protocol did not allow more explicit modeling. The model using these assumptions could describe the data well. The effect of these assumptions is, however, not entirely clear and needs to be further investigated.

Our presented method to improve the BED to the tumor could be applied to other therapies with radiolabeled peptides or antibodies, for example, to ^{177}Lu-labeled peptides, for which less kidney toxicity was observed.

To further validate the presented approach, different amounts of peptide and pertaining activities could be administered in the same patient for various cycles or in similar patients.

CONCLUSION

The results of this work based on PBPK modeling suggest that in PRRT with ^{90}Y-DOTATATE the effect of peptide amount on the tumor-to-kidney BED ratio is substantial in most patients and therefore needs to be considered in PRRT. For the investigated patients, the optimal administered peptide amount and the pertaining activity could be identified. In particular, the absorbed doses to poorly perfused tumors (or tumor regions) with average to high receptor concentration might be considerably improved. The proposed treatment planning method might also be important for other therapies using radiolabeled ligands. The PBPK model can be adapted to other peptides such as prostate-specific membrane antigen ligands while using the same algorithm to find the individual optimal combination of activity and amount.

DISCLOSURE

The costs of publication of this article were defrayed in part by the payment of page charges. Therefore, and solely to indicate this fact, this article is hereby marked "advertisement" in accordance with 18 USC section 1734. This work was supported by the Deutsche Forschungsgemeinschaft (DFG KL 2742/2-1, BE 4393/1-1 and GL 236/11-1). No other potential conflict of interest relevant to this article was reported.

REFERENCES

1. Pool SE, Krenning EP, Koning GA, et al. Preclinical and clinical studies of peptide receptor radionuclide therapy. *Semin Nucl Med.* 2010;40:209–218.
2. Bodei L, Müller-Brand J, Baum RP, et al. The joint IAEA, EANM, and SNMMI practical guidance on peptide receptor radionuclide therapy (PRRNT) in neuroendocrine tumours. *Eur J Nucl Med Mol Imaging.* 2013;40:800–816.
3. Cremonesi M, Ferrari M, Di Dia A, et al. Recent issues on dosimetry and radiobiology for peptide receptor radionuclide therapy. *Q J Nucl Med Mol Imaging.* 2011;55:155–167.
4. Müller C, Forrer F, Bernard BF, et al. Diagnostic versus therapeutic doses of [^{177}Lu-DOTA-Tyr$_3$]-octreotate: uptake and dosimetry in somatostatin receptor-positive tumors and normal organs. *Cancer Biother Radiopharm.* 2007;22:151–159.
5. de Jong M, Breeman WA, Bernard BF, et al. Tumour uptake of the radiolabelled somatostatin analogue [DOTA0, TYR3]octreotide is dependent on the peptide amount. *Eur J Nucl Med.* 1999;26:693–698.
6. Kletting P, Bunjes D, Reske SN, Glatting G. Improving anti-CD45 antibody radioimmunotherapy using a physiologically based pharmacokinetic model. *J Nucl Med.* 2009;50:296–302.
7. Kletting P, Bunjes D, Luster M, Reske SN, Glatting G. Optimal preloading in radioimmunotherapy with anti-CD45 antibody. *Med Phys.* 2011;38:2572–2578.
8. Kletting P, Maass C, Reske S, Beer AJ, Glatting G. Physiologically based pharmacokinetic modeling is essential in ^{90}Y-labeled anti-CD66 radioimmunotherapy. *PLoS One.* 2015;10:e0127934.
9. Kletting P, Muller B, Erentok B, et al. Differences in predicted and actually absorbed doses in peptide receptor radionuclide therapy. *Med Phys.* 2012;39:5708–5717.
10. Sabet A, Nagarajah J, Dogan AS, et al. Does PRRT with standard activities of ^{177}Lu-octreotate really achieve relevant somatostatin receptor saturation in target tumor lesions?: insights from intra-therapeutic receptor imaging in patients with metastatic gastroenteropancreatic neuroendocrine tumors. *EJNMMI Res.* 2013;3:82.
11. Malik N, Machulla H, Reske S, Solbach C. Radiosynthesis of [^{90}Y]DOTA-DUPA-Pep for clinical applications [abstract]. *J Nucl Med.* 2014;55(suppl 1):1149.
12. de Jong M, Bakker WH, Krenning EP, et al. Yttrium-90 and indium-111 labelling, receptor binding and biodistribution of [DOTA0,d-Phe1,Tyr3]octreotide, a promising somatostatin analogue for radionuclide therapy. *Eur J Nucl Med.* 1997;24:368–371.
13. Glatting G, Landmann M, Kull T, et al. Internal radionuclide therapy: the UlmDos software for treatment planning. *Med Phys.* 2005;32:2399–2405.
14. Kletting P, Schimmel S, Hanscheid H, et al. The NUKDOS software for treatment planning in molecular radiotherapy. *Z Med Phys.* 2015;25:264–274.
15. Siegel JA, Thomas SR, Stubbs JB, et al. MIRD pamphlet no. 16: techniques for quantitative radiopharmaceutical biodistribution data acquisition and analysis for use in human radiation dose estimates. *J Nucl Med.* 1999;40:37S–61S.
16. Boy C, Heusner TA, Poeppel TD, et al. ^{68}Ga-DOTATOC PET/CT and somatostatin receptor (sst1-sst5) expression in normal human tissue: correlation of sst2 mRNA and SUV(max). *Eur J Nucl Med Mol Imaging.* 2011;38:1224–1236.
17. Reubi JC, Schar JC, Waser B, et al. Affinity profiles for human somatostatin receptor subtypes SST1-SST5 of somatostatin radiotracers selected for scintigraphic and radiotherapeutic use. *Eur J Nucl Med.* 2000;27:273–282.
18. Krenning EP, Bakker WH, Kooij PPM, et al. Somatostatin receptor scintigraphy with indium-111-DTPA-D-PHe-1-octreotide in man: metabolism, dosimetry and comparison with iodine-123-tyr-3-octreotide. *J Nucl Med.* 1992;33:652–658.
19. Froidevaux S, Eberle AN, Christe M, et al. Neuroendocrine tumor targeting: study of novel gallium-labeled somatostatin radiopeptides in a rat pancreatic tumor model. *Int J Cancer.* 2002;98:930–937.
20. Schmidt MM, Wittrup KD. A modeling analysis of the effects of molecular size and binding affinity on tumor targeting. *Mol Cancer Ther.* 2009;8:2861–2871.
21. Antunes P, Ginj M, Zhang H, et al. Are radiogallium-labelled DOTA-conjugated somatostatin analogues superior to those labelled with other radiometals? *Eur J Nucl Med Mol Imaging.* 2007;34:982–993.
22. Kimura H, Takeuchi H, Koshimoto Y, et al. Perfusion imaging of meningioma by using continuous arterial spin-labeling: comparison with dynamic susceptibility-weighted contrast-enhanced MR images and histopathologic features. *AJNR.* 2006;27:85–93.
23. Guyennon A, Mihaila M, Palma J, Lombard-Bohas C, Chayvialle JA, Pilleul F. Perfusion characterization of liver metastases from endocrine tumors: computed tomography perfusion. *World J Radiol.* 2010;2:449–454.
24. Barrett PH, Bell BM, Cobelli C, et al. SAAM II: simulation, analysis, and modeling software for tracer and pharmacokinetic studies. *Metabolism.* 1998;47:484–492.
25. Glatting G, Kletting P, Reske SN, Hohl K, Ring C. Choosing the optimal fit function: comparison of the Akaike information criterion and the F-test. *Med Phys.* 2007;34:4285–4292.
26. Kletting P, Schimmel S, Kestler HA, et al. Molecular radiotherapy: the NUKFIT software for calculating the time-integrated activity coefficient. *Med Phys.* 2013;40:102504.
27. Burnham KP, Anderson DR. *Model Selection and Multimodel Interference: A Practical Information-Theoretic Approach.* 2nd ed. New York, NY: Springer; 2002.
28. Cremonesi M, Botta F, Di Dia A, et al. Dosimetry for treatment with radiolabelled somatostatin analogues. A review. *Q J Nucl Med Mol Imaging.* 2010;54:37–51.
29. Baechler S, Hobbs RF, Prideaux AR, Wahl RL, Sgouros G. Extension of the biological effective dose to the MIRD schema and possible implications in radionuclide therapy dosimetry. *Med Phys.* 2008;35:1123–1134.
30. Vinjamuri S, Gilbert TM, Banks M, et al. Peptide receptor radionuclide therapy with ^{90}Y-DOTATATE/^{90}Y-DOTATOC in patients with progressive metastatic neuroendocrine tumours: assessment of response, survival and toxicity. *Br J Cancer.* 2013;108:1440–1448.
31. Stabin MG, Sparks RB, Crowe E. OLINDA/EXM: the second-generation personal computer software for internal dose assessment in nuclear medicine. *J Nucl Med.* 2005;46:1023–1027.
32. Konijnenberg M. From imaging to dosimetry and biological effects. *Q J Nucl Med Mol Imaging.* 2011;55:44–56.
33. Dale RG. The application of the linear-quadratic dose-effect equation to fractionated and protracted radiotherapy. *Br J Radiol.* 1985;58:515–528.
34. Soto-Montenegro ML, Pena-Zalbidea S, Mateos-Perez JM, et al. Meningiomas: a comparative study of ^{68}Ga-DOTATOC, ^{68}Ga-DOTANOC and ^{68}Ga-DOTATATE for molecular imaging in mice. *PLoS One.* 2014;9:e111624.
35. Velikyan I, Sundin A, Eriksson B, et al. In vivo binding of [^{68}Ga]-DOTATOC to somatostatin receptors in neuroendocrine tumours–impact of peptide mass. *Nucl Med Biol.* 2010;37:265–275.
36. Vaupel P, Kallinowski F, Okunieff P. Blood flow, oxygen and nutrient supply, and metabolic microenvironment of human tumors: a review. *Cancer Res.* 1989;49:6449–6465.